

Human Cingulate and Paracingulate Sulci: Pattern, Variability, Asymmetry, and Probabilistic Map

Tomáš Paus,¹ Francesco Tomaiuolo,² Naim Otaky,¹ David MacDonald,¹ Michael Petrides,¹ Jason Atlas,¹ Renée Morris,¹ and Alan C. Evans¹

¹Montreal Neurological Institute, McGill University, Montreal, Canada, and ²Istituto di Fisiologia Umana, Università di Verona, Verona, Italy

Recent advances in functional neuroimaging of the human cerebral cortex revived interest in the study of the cortical morphology at both macro- and microscopic levels. By means of high-resolution magnetic resonance imaging (MRI), *in vivo* images of the human brain can be acquired and used to aid localization of the functional maps. The goal of the present study was to determine variability in the occurrence and location of the cingulate sulcus (CS) and the paracingulate sulcus (PCS). Brain MRIs of 247 healthy young volunteers were obtained and transformed into a standardized stereotaxic space (Talairach and Tournoux, 1988). The CS and PCS were marked in 494 hemispheres using software capable of real-time movement through a 3-D volume. The markers were used to generate a probabilistic map of the CS and PCS. The individual MRI images were also evaluated for the presence and location of the following morphological features: the continuity of the CS, the presence of vertically oriented branches of the CS, the presence of the PCS, and the presence of the intralimbic sulcus. The results revealed considerable variability in the location of some of the above morphological features and a striking hemispheric asymmetry in the prominence of the PCS. The results of four previous blood-flow activation studies of speech control were used to illustrate the relevance of our morphological findings for functional neuroimaging of the human anterior cingulate cortex.

The study of the cerebral sulci of the human brain was entertained by many anatomists at the end of the last and the beginning of this century. The main emphasis was on the description of the sulcal pattern, its variability and asymmetries between the left and right hemispheres (Eberstaller, 1884; Retzius, 1896; Weinberg, 1905). The development of staining techniques shifted the interest toward the cellular and fiber composition of the cerebral cortex and the delineation of myelo- and cytoarchitectonic areas (Brodmann, 1909; Vogt and Vogt, 1919; Economo and Koskinas, 1925; Bailey and Bonin, 1951; Sarkissov et al., 1955). The relationship between the macro- and microscopic morphological features, namely between the cerebral sulci and the cyto- and/or myeloarchitectonic borders, was pointed out in some of the early studies (e.g., Smith, 1907; Sanides, 1964) and reexamined recently by Rademacher et al. (1993).

Recent advances in functional neuroimaging (see Raichle, 1987; Binder and Rao, 1994) together with the availability of high-resolution structural magnetic resonance images (MRI)¹ revived interest in mapping structural features of the human cerebral cortex. One of the reasons for this interest is the desire to correlate functional maps with those of the underlying structure in order to standardize functional localization and allow cross-technique (and cross-species) integration of data from different studies. However, *in vivo* imaging techniques are not, at present, capable of providing structural maps of the human cerebral cortex that would reveal differences in the cyto-, myelo-, or chemoarchitecture (but see Clark et al., 1992). Cerebral sulci may, in this respect, provide the missing reference point and thus aid comparisons between the functional and detailed structural maps of the cerebral cortex.

Description of the sulcal pattern and its variability in a large sample of individuals could be a first step toward identifying morphological landmarks potentially useful for correlating functional and structural maps. Ono et al. (1990), using a limited set of 25 brain specimens, described different variants of the primary and secondary sulci of the human cerebral cortex. In the present study, we have focused on the sulcal pattern of the medial wall of the frontal lobe. The main sulcus in this region is the cingulate sulcus (CS), which courses around the corpus callosum and extends posteriorly into the parietal lobe as the marginal ramus (see Fig. 1). Dorsal to the anterior portion of the CS, another sulcus is often present. This sulcus, which is not usually identified in standard neuroanatomy textbooks, was referred to by Elliot Smith as the paracingulate sulcus (Smith, 1907). The presence and the course of both the cingulate and the paracingulate (PCS) sulci were examined in 247 brain MRIs of young healthy volunteers. The location of several morphological landmarks in this region was specified within a standardized stereotaxic space (Talairach and Tournoux, 1988), thus allowing direct reference to the results of functional neuroimaging studies. Inter-individual variability of the sulcal pattern, left-right asymmetry, and gender differences were also evaluated. Finally, a three-dimensional probabilistic map of the cingulate and the paracingulate sulci was created that provides coordinates of the average ($n = 247$) cingulate and paracingulate sulci in the standardized stereotaxic space.

A preliminary report of this study has been presented elsewhere in abstract form (Tomaiuolo et al., 1993).

Materials and Methods

The MRIs were obtained in a total of 305 subjects; 247 MRIs of sufficient quality were used in the present analysis (60 females: age range, 18–33 years; mean \pm SD, 22.6 ± 3.6 years; 187 males: age range, 16–41 years; mean \pm SD, 23.9 ± 4.4 years). The primary purpose for acquiring the MRIs was that of structural correlation with functional images obtained with positron emission tomography (Evans et al., 1991). Subjects whose MRIs are included in this report volunteered for blood-flow activation studies carried out at the McConnell Brain Imaging Center, Montreal Neurological Institute, between August 1989 and June 1992. In order to participate in the activation study, the subject had to be right-handed and had to have a negative history of neurologic and/or psychiatric disorders.

All MRI scans were performed on a Philips Gyroscan 1.5-T superconducting magnet system. Using multiplanar spin-echo acquisition, 64 contiguous T₁-weighted (T_R = 550 msec, T_E = 30 msec) 2 mm thick slices were collected in the axial plane. The MRI images were first resampled by interpolation to a standardized space (Talairach and Tournoux, 1988), resulting in a volume of 160 axial slices with an in-plane matrix of 256 by 256 pixels. The thicknesses of the interpolated sagittal, coronal, and axial slices were 0.67, 0.86, and 0.75 mm, respectively. The transformation to the standardized space was based on the identification of the line passing through the anterior and posterior commissures (the AC-PC line) and on the measurement of three scaling factors accounting for brain size (Evans et al., 1992).

With an interactive 3-D software package capable of real-time tri-

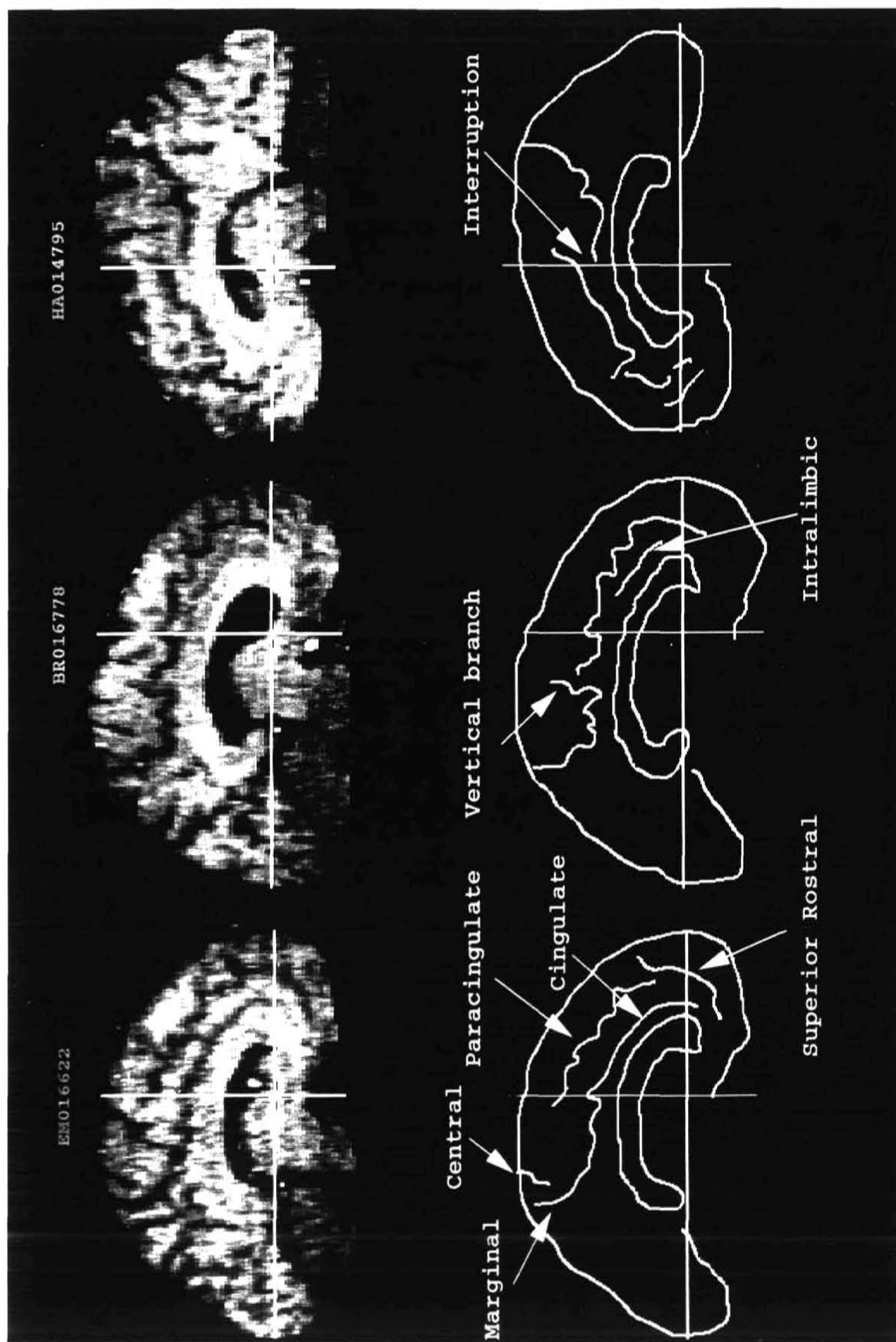


Figure 1. Magnetic resonance images of two left hemispheres (subjects EM016622 and BR016778) and one right (subject HA014795) hemisphere (top) and the corresponding line drawings (bottom) are shown to illustrate the following morphological features: central, central sulcus; cingulate, cingulate sulcus; intralimbic, interruption of the cingulate sulcus; marginal, marginal ramus of the cingulate sulcus; paracingulate, paracingulate sulcus; superior rostral, superior rostral sulcus; vertical branch, vertically oriented branch of the cingulate sulcus. The vertical ($Y = 0$) and horizontal ($Z = 0$) planes passing through the anterior commissure are marked by the vertical and horizontal lines, respectively. The images were transformed into standardized stereotaxic space (Talairach and Tournoux, 1988).

Table 1
Segmentation of the cingulate sulcus

	One segment	Two segments	Three segments
Left hemisphere	215 (87)	30 (12)	2 (1)
Right hemisphere	197 (80)	47 (19)	3 (1)

Data are absolute number of hemispheres; incidence rates (%) are given in parentheses.

plane movement through a 3-D volume, the CS and PCS were marked in 494 hemispheres (247 brains). The sulci were identified on 0.67 mm thick sagittal sections as sets of 3-D voxels of visually apparent contrast between the gray and the white matter (up to 30 adjacent sagittal sections per hemisphere). The axial and coronal sections were used to confirm the correct placement of voxel labels for each sulcus. On average, 900 markers per hemisphere were used to represent the sulci. The markers were subsequently used to create a probabilistic map of the CS and PCS (defined below).

The following morphological features were evaluated on each of the individual MRIs: the continuity of the CS, the presence of vertically oriented branches of the CS, the presence of the paracingulate sulcus, and the presence of the intralimbic sulcus (see Fig. 1). The CS was considered continuous unless there was a clear interruption (gap of more than 10 mm) present on several adjacent sagittal sections. The incidence and location of such interruptions were recorded. A "branch" of the CS was defined as a vertically oriented element of at least 10 mm in length; the element had to show continuity with the CS. The incidence and location of the branches were recorded. The paracingulate sulcus was defined as the sulcus located dorsal to the CS with a course parallel to the CS. The appearance of the PCS was classified into three categories: prominent, present, and absent. The PCS was described as prominent if it consisted of one or more clearly developed horizontal elements that formed a sulcus, parallel to the CS, of at least 20 mm in length. The PCS was described as present if there were several vertically oriented elements in the PCS region with no spatial relationship to the CS. The intralimbic sulcus was defined as the shallow sulcus between the CS and the supracallosal sulcus. The incidence of the PCS and that of the intralimbic sulcus were calculated.

A probabilistic map (i.e., a 3-D image of the likelihood that any 3-D pixel in stereotaxic space will be labeled as including the relevant sulcus) was produced in the following way. First, a dilation operation was performed around each landmark to generate a solid 3-D object representing each sulcus. Second, these objects were averaged within the standardized stereotaxic space across all subjects ($n = 247$).

Results

The cingulate sulcus was invariably present in all the hemispheres studied. In the majority of cases, the caudal end of the CS (i.e., the marginal ramus) was located just behind the medial portion of the central sulcus.² Starting from the marginal ramus, the CS sweeps forward around the corpus callosum (CC). The rostral end of the CS extended to the level of the genu of the CC, where it either tapered off or fused with the superior rostral sulcus. The fusion with the superior rostral sulcus occurred either in front of or ventral to the genu of the CC. In most cases, the CS was uninterrupted. However, a small but significant number of hemispheres contained a CS divided into two or three distinct segments (Table 1). Along its course, the CS frequently gave off one or more

Table 2
Vertically oriented branches of the cingulate sulcus

	No branch	One	Two	Three	Four
Left hemisphere	54 (22)	112 (45)	70 (28)	11 (5)	0 (0)
Right hemisphere	47 (19)	100 (41)	77 (31)	21 (8)	2 (1)

Data are absolute number of hemispheres with a given number of branches; incidence rates (%) are given in parentheses.

Table 3
Frequency of the occurrence and type of the paracingulate sulcus

	Prominent	Present	Absent
Left hemisphere	134 (54)	93 (38)	20 (8)
Right hemisphere	91 (37)	119 (48)	37 (15)

Data are absolute number of hemispheres; incidence rates (%) are given in parentheses.

vertically oriented "branches" (Table 2). In addition to the primary cingulate sulcus, two secondary sulci were also observed: the paracingulate sulcus and the intralimbic sulcus. The PCS was, in more or less developed form, present in the majority of cases (Table 3), whereas the intralimbic sulcus was very rare in its occurrence (Table 4).

Location of CS Interruptions and CS Branches

The location of two morphological features, the presence of interruption and a vertical branch, was specified along the anterior-posterior axis by the Y coordinate (Talairach and Tournoux, 1988). As can be seen in Figure 2A, which contains a frequency histogram of Y coordinates of the interruption in hemispheres with the two-segment CS, the interruption occurs most frequently within ± 15 mm of the vertical plane defined by the anterior commissure ($Y = 0$). The frequency histogram (Y coordinates) for the first vertical branch after the marginal ramus is presented in Figure 2B. The histogram has a bimodal distribution, suggesting the presence of two distinct types of branches: a caudal branch, which occurs most frequently between $Y = -20$ mm and $Y = -10$ mm, and a rostral branch with the maximum occurrence between $Y = -5$ mm to $Y = +5$ mm. The location of the second branch (see Fig. 2C) supports the distinction between the caudal and rostral branches in that its frequency histogram overlaps with the "rostral" portion of the histogram for the first branch. Thus, in some cases the CS gives off both rostral and caudal branches, whereas in other cases the caudal branch is absent.

Left-Right Asymmetries

Hemispheric asymmetry was evaluated for the following morphological features: (1) segmentation of the CS, (2) number of vertically oriented CS branches, (3) presence (and type) of the paracingulate sulcus, and (4) presence of the intralimbic sulcus. The statistical significance of the differences, was assessed by means of a modified χ^2 with Yates's correction.

The left CS was divided into one or more distinct segments less frequently than the right CS [$\chi^2(2) = 9.5, p = 0.009$]. The left CS, as compared with the right CS, also gave off a lower number of vertically oriented branches [$\chi^2(4) = 11.9, p = 0.002$]. On the other hand, the well-developed paracingulate sulcus was more frequently present in the left than in the right hemisphere [$\chi^2(2) = 16.8, p = 0.0002$]. There was no significant left-right difference in the presence of the intralimbic sulcus [$\chi^2(1) = 1.1, p = 0.3$].

Gender Differences

Gender effect was evaluated for the same morphological features evaluated for the left-right hemispheric asymmetry (see

Table 4
Frequency of the occurrence of the intralimbic sulcus

	Present	Absent
Left hemisphere	10 (4)	237 (96)
Right hemisphere	14 (6)	233 (94)

Data are absolute number of hemispheres; incidence rates (%) are given in parentheses.

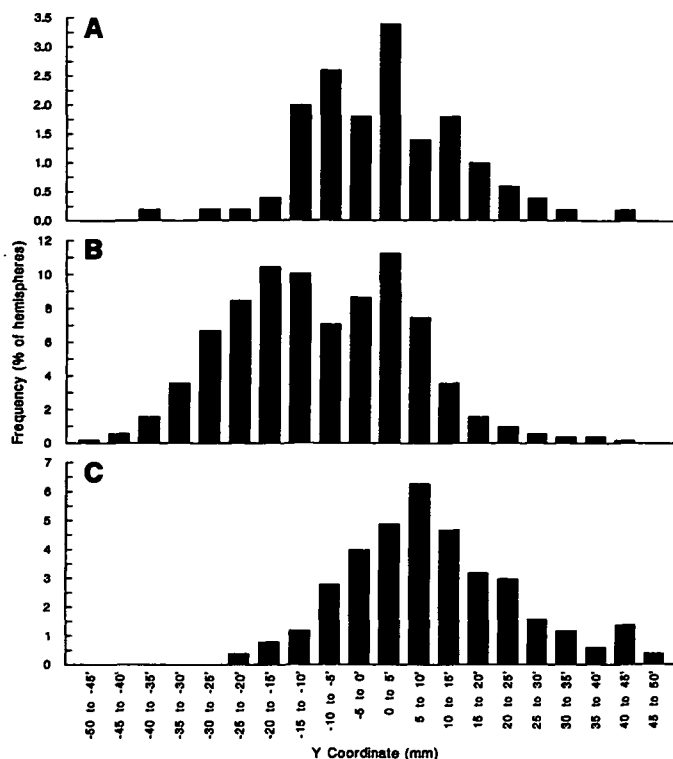


Figure 2. A frequency histogram of Y coordinates for the CS interruption (A), the first CS branch (B), and the second CS branch (C). An interruption was defined as a gap of more than 10 mm. A branch of the CS was defined as a vertically oriented element of at least 10 mm in length. The order of branches (i.e., the first, second, etc.) was counted from the marginal ramus forward.

above). The statistical significance of the differences between females and males was first evaluated irrespective of the hemispheric differences by means of a modified χ^2 with Yates's correction. Subsequently, gender (male or female) by hemisphere (left or right) interactions were assessed by means of a log-linear analysis.

There were no significant gender differences in the number of CS segments, number of CS branches, or the incidence of the intralimbic sulcus. The only significant gender effect was that of a difference in distribution of the prominent, present, and absent paracingulate sulcus in males and females [$\chi^2(2) = 7.7, p = 0.02$]. This effect reflects a higher incidence of the two extreme categories of the PCS, namely, the prominent and the absent PCS, in females. The frequency of the prominent, present, and absent PCS, respectively, was 50, 33, and 17% in females, and 44, 46, and 10% in males. The log-linear analysis of the gender-by-hemisphere interaction did not reveal significant effects on either the type of the PCS or on any other morphological feature examined.

Probabilistic Map

The probabilistic map of the CS and PCS is shown on Figure 3. A clear left-right asymmetry can be seen on the map in that the left PCS has an overall higher probability than the right PCS. The location of the two sulci in the standardized space may be approximated by means of the grid that indicates the Y and Z coordinates.

Discussion

Our analysis of 247 brain MRIs revealed a considerable variability in the sulcal pattern on the medial wall of the frontal lobe. The sulci in this region differ from person to person in

the continuity of the cingulate sulcus, number and location of vertically oriented branches of the CS, and the presence or absence of the paracingulate sulcus. Significant asymmetries exist between the left and right hemispheres at this gross morphological level. In the following discussion, we shall first compare our results with those of previous descriptive studies. Then, we shall comment briefly on the possible spatial relationship between some of the morphological landmarks and the cortical architecture. Finally, the relevance of the current study to the issue of functional localization will be illustrated.

In this study, the cingulate sulcus was observed to be continuous in over 80% of the hemispheres. This is in sharp contrast to previous reports by Ono et al. (1990), Weinberg (1905), and Retzius (1896), who found the contiguous CS in only 58, 54, and 41% hemispheres, respectively. The discrepancy is probably related to the type of material (autopsy specimen vs MRI) and our rather conservative definition of the interruption (10 mm gap). It is important to note that most interruptions identified in this study were of the "posterior" type (see Ono et al., 1990, their Fig. 13.1). The incidence rates of this type of interruption in the Ono et al. material are not different from that reported in our study (Ono et al., 1990: left, 12%; right, 24%; this study: left, 12%; right, 22%). Thus, the overall low number of the CS interruptions reported in our study is probably due to the underreporting of the anterior type of interruption. This, in turn, may be related to the ambiguity of the sulcal pattern in the region just in front of the genu of the corpus callosum (where there is a confluence of the CS, PCS, and the superior rostral sulcus).

The frequent presence of vertically oriented branches of the CS reflects the relative overgrowth of the cortical matter in the human brain as compared with that of nonhuman primates (see Zilles et al., 1989, for a comparative study of gyrification in primates). In our sample, only 44% (left) and 30% (right) hemispheres did not give off a vertical branch longer than 10 mm. The incidence of a CS without branches is comparable to that reported by Weinberg (1905), namely, 32% hemispheres with the CS without a branch. The caudal branch (i.e., the branch located behind the vertical plane defined by the anterior commissure) may be analogous to the paracentral sulcus defined by Ono et al. (1990, their Fig. 13.64). In the hemispheres with the posterior interruption of the CS, the caudal branch often formed a vertically oriented extension of the posterior segment of the CS (see Fig. 1, case BR016778). This pattern was also noted by Ono et al. 1990 (see Ono et al., 1990, their Fig. 13.6D). It could be that the caudal branch and/or the caudal interruption coincides with a zone of transition between the posterior (Brodmann's area 23) and anterior (area 24) cingulate cortex.

The higher incidence of the paracingulate sulcus in the left hemisphere was the most striking asymmetry found in our material. Such asymmetry was not observed by Ono et al. (1990), but was described by Weinberg (1905). Note that both these authors refer to the PCS as a doubling of the CS in its anterior part. Weinberg (1905) reported the presence of the "doubling of the cingulate sulcus in its anterior part" in 84% left and 40% right hemispheres as compared with the presence of the prominent PCS in 54 and 37% of the left and right hemispheres, respectively, in our sample. The presence of the prominent PCS in the left hemisphere can be seen clearly on the probabilistic map (Fig. 3) as a second ridge of density dorsal to the CS. The better-developed PCS in the left hemisphere may reflect relative expansion of the left paralimbic cortex (Brodmann's area 32). In primates, at least a portion of area 32 is involved in vocalization (Vogt and Barbas, 1988, see below for the relevant blood-flow activation data). A major source of sensory input into this brain region comes

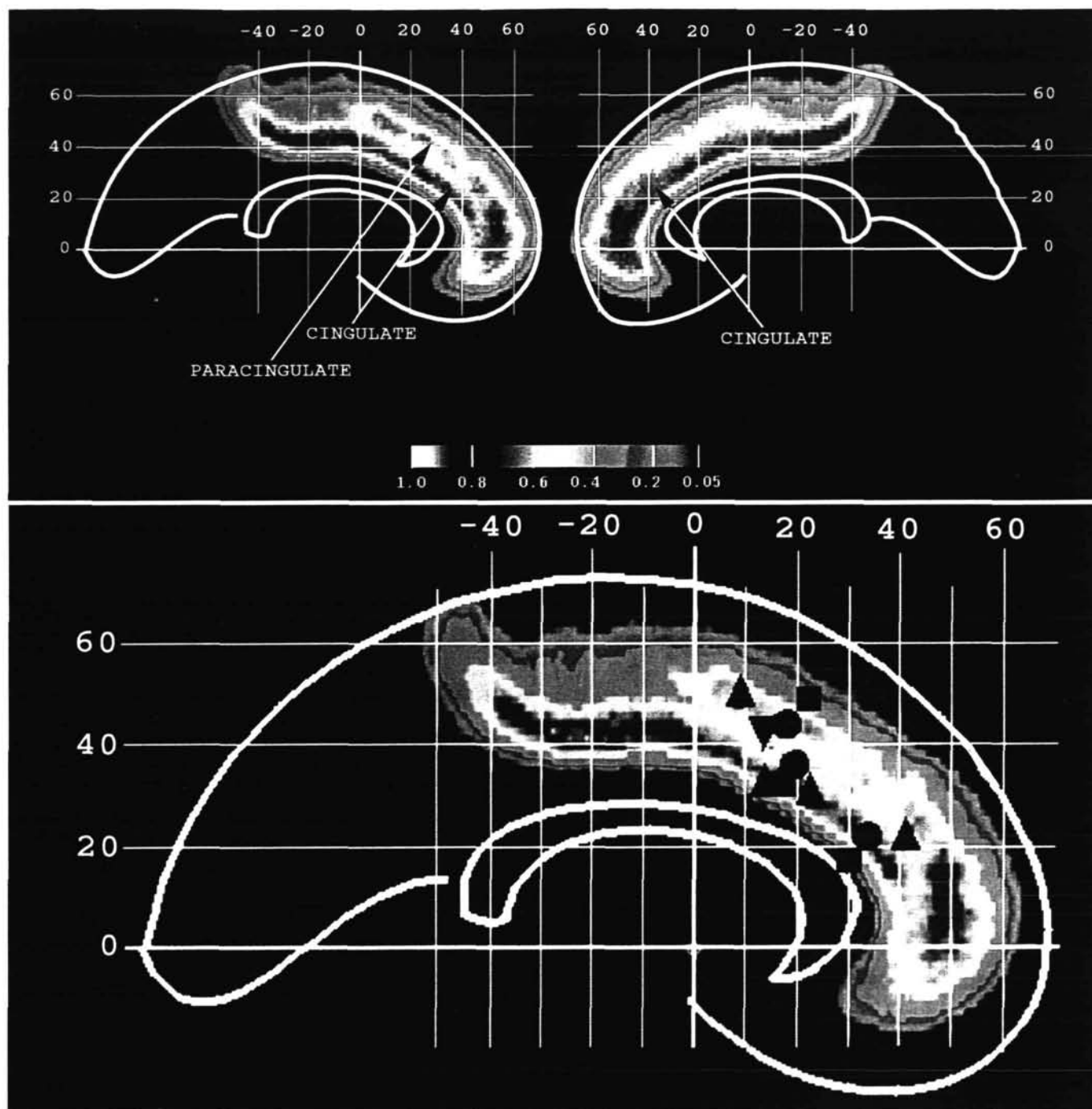


Figure 3. Sagittal sections through the probabilistic map of the cingulate and paracingulate sulcus. The sections pass 7 mm to the left and right from the midsagittal plane. The probabilistic map, the brain outlines, and the grid are all placed in the standardized space (Talairach and Tournoux, 1988). Numbers corresponding to the vertical and horizontal lines indicate distances (in mm) from the vertical and horizontal planes defined by the anterior commissure, respectively. The color scale codes the likelihood that any 3-D pixel in stereotaxic space will be labeled as including the relevant sulcus (see Materials and Methods for details).

Figure 5. Localization of activation peaks on the probabilistic map of the cingulate and paracingulate sulci. The locations (Y and Z coordinates) of 11 peaks obtained in four blood-flow activation studies were projected onto the sagittal section passing 7 mm to the left of the midline. Both the left-hemisphere (X < 0) and right-hemisphere (X > 0) peaks were projected on the left probabilistic map. Note the close spatial relationship between the dorsal group of peaks (Z > 40) and the paracingulate sulcus, the ventral group of peaks (Z < 40) and the cingulate sulcus, and the rostral group of peaks and the anterior end of the cingulate sulcus. In all four studies, the peak corresponds to the site of the maximal statistical difference between two group averages of cerebral blood-flow images obtained during the performance of automatic and effortful speech tasks, respectively. Peaks marked by squares were obtained in the Reversal minus Overpracticed subtraction in Paus et al. (1993, experiment 1) (-1 22 49, -4 30 17). Peaks marked by circles were also obtained in the Reversal minus Overpracticed subtraction, but in another group of subjects (Paus et al., 1993, experiment 3) (3 18 44, 5 20 36, 7 34 22). The triangles mark peaks found in the study of Pardo et al., 1990 (Incongruent minus Congruent condition of the Stroop test; 7 9 49, 7 15 32, 10 17 32, 17 23 30, -13 41 21). The triangle with the base up indicates a peak reported by Taylor et al. (1994) (-10 14 43) for an Incongruent minus Congruent subtraction used in a modified Stroop test. Numbers in parentheses are the X, Y, and Z coordinates, respectively, of the plotted activation peaks. Numbers corresponding to the vertical and horizontal lines indicate distances (in mm) from the vertical (Y) and horizontal (Z) planes, respectively, defined by the anterior commissure.

activation peaks on the probabilistic map of the left cingulate and paracingulate sulci. We decided to project both the left and right activation peaks on the left probabilistic map in order to demonstrate more clearly the spatial relationship between the peaks and the two sulci. We would also argue that it is difficult to determine whether a cingulate peak falls within the left or right hemisphere unless the distance from the midline is at least 6 mm. As can be seen on Figure 5, four activation peaks are located in the proximity of the paracingulate sulcus, another four peaks are located more ventrally near the cingulate sulcus, and three additional peaks were found close to the anterior end of the cingulate sulcus. It is unclear whether the two caudal groups of peaks (Y , 9–23 mm) represent two distinct functional regions or simply reflect between-study variability in the absolute localization. On the other hand, it is evident that the rostral group of activation peaks is separate in its localization from the two caudal groups. In fact, in our studies (Paus et al., 1993), the paracingulate and the rostral-cingulate peaks were obtained from the same subtractions, suggesting concomitant activation of the two regions. The spatial relationship between the activation peaks and the sulci supports the notion of two distinct speech-related regions in the human anterior cingulate cortex (Paus et al., 1993), namely, the anatomically defined Brodmann's area 32, which coincides with the paracingulate region, and the rostral portion of area 24, which is located at the rostral end of the cingulate sulcus. This view is consistent with the known structural and functional organization of the monkey cingulate cortex with regard to vocalization (Smith, 1941; Sutton et al., 1974; Muakkassa and Strick, 1979; Aitken, 1981; Barbas, 1988; McLean and Newman, 1988; Vogt and Barbas, 1988; Morecraft and Van Hoesen, 1992; Bates and Goldman-Rakic, 1993).

In conclusion, our study defined the extent of morphological variability in the pattern and location of the human cingulate and paracingulate sulci in a large sample of 494 hemispheres. Subsequent studies are required to clarify the spatial relationship between some of the morphological landmarks and the cortical architecture. Morphometric studies are needed to confirm the observed hemispheric asymmetry for the presence of the paracingulate sulcus and the gender differences in the prominence of this sulcus. Single-subject studies, using positron emission tomography and/or functional MRI, will also corroborate possible spatial relationships between the structural and functional maps in the cingulate region.

Notes

1. High-resolution MRI is an excellent tool for the morphometric analysis of the human cerebral cortex. Various methods have been developed and applied in a limited number of structures (Filipek et al., 1989; Vannier et al., 1991; Lancaster et al., 1992; Rademacher et al., 1992; Andreasen et al., 1994).

2. The relative position of the marginal ramus and the medial portion of the central sulcus was examined in 92 hemispheres. In only two hemispheres was the central sulcus located behind the marginal ramus. In over 50% of the hemispheres, the marginal ramus was found 10 to 15 mm behind the central sulcus. This was equally true for the left and right hemispheres.

3. Because of differences in the definition of the $Y = 0$ plane and the z_{\max} (the height of the brain) in the two versions of the Talairach stereotaxic atlas (Talairach et al., 1967; Talairach and Tournoux, 1988), the following corrections were made. In the report of Pardo et al. (1990), $Y = 0$ was defined as halfway between the anterior and posterior commissures, according to Talairach et al. (1967). In the other studies, $Y = 0$ was defined at the level of the anterior commissure, according to Talairach and Tournoux (1988). Thus, the difference between the two planes represents half of the distance between the commissures (i.e., approximately 12 mm). For consistency across studies, the Y coordinates reported in the study by Pardo et al. (1990) were recomputed by subtracting 12 mm from the value of

the Y coordinates given in the original study. Furthermore, due to the lower value of the z_{\max} used in the Pardo et al. (1990) study, as compared to the z_{\max} value used in the Paus et al. (1993) and Taylor et al. (1994) studies, the z coordinates given in the original report of Pardo et al. (1990) were recomputed by multiplying the original values by a factor of 1.07 ($z_{\max} = 70$ mm and $z_{\max} = 75$ mm in the 1967 and the 1988 Talairach stereotaxic atlases, respectively).

This work was supported by the McDonnell-Pew Program in Cognitive Neuroscience, the International Consortium for Brain Mapping, the Human Brain Map Project, the Medical Research Council (Canada), and the Natural Sciences and Engineering Research Council (Canada). We thank Dr. B. Milner for her comments on the manuscript and two anonymous reviewers for helpful suggestions. R. Amsel and J. Kaczorowski provided advice regarding the statistical treatment of the data.

Address correspondence to Dr. Tomás Paus, Montreal Neurological Institute, 3801 University Street, Montreal, Quebec, H3A 2B4, Canada.

References

- Aitken PG (1981) Cortical control of conditioned and spontaneous vocal behavior in rhesus monkeys. *Brain Lang* 13:171–184.
- Andreasen NC, Harris G, Cizadilo T, Arndt S, O'Leary DS, Swayze V, Flaum M (1994) Techniques for measuring sulcal/gyral patterns in the brain as visualized through magnetic resonance scanning: BRAINPLOT and BRAINMAP. *Proc Natl Acad Sci USA* 90:93–97.
- Bailey P, Bonin G (1951) The isocortex of man. Urbana, IL: University of Illinois.
- Barbas H (1988) Anatomic organization of basoventral and medio-dorsal visual recipient prefrontal regions in the rhesus monkey. *J Comp Neurol* 276:313–342.
- Bates JF, Goldman-Rakic PS (1993) Prefrontal connections of medial motor areas in the rhesus monkey. *J Comp Neurol* 336:211–228.
- Binder JR, Rao SM (1994) Human brain mapping with functional magnetic resonance imaging. In: Localization and neuroimaging in neuropsychology (Kertesz A, ed), pp 185–212. Orlando, FL: Academic.
- Brodman K (1909) Vergleichende Lokalisationslehre der Großhirnrinde. Leipzig: Barth.
- Clark VP, Courchesne E, Grafe M (1992) *In vivo* myeloarchitectonic analysis of human striate and extrastriate cortex using magnetic resonance imaging. *Cereb Cortex* 2:417–424.
- Eberstaller O (1884) Zur Oberflächenanatomie der Grosshirn-hemisphären. *Wien Med Blätter* 7:479–482, 542–582, 644–646.
- Economo C, Koskinas GN (1925) Die Cytoarchitektonik der Hirnrinde des erwachsenen Menschen. Berlin: Springer.
- Evans AC, Marrett S, Torrescorzo J, Ku S, Collins L (1991) MRI-PET correlative analysis using a volume of interest (VOI) atlas. *J Cereb Blood Flow Metab* 11:A69–A78.
- Evans AC, Marrett S, Neelin P, Collins L, Worsley K, Dai W, Milot S, Meyer E, Bub D (1992) Anatomical mapping of functional activation in stereotactic coordinate space. *NeuroImage* 1:43–53.
- Filipek PA, Kennedy DN, Caviness VS Jr, Rossnick SL, Spraggins TA, Starewicz PM (1989) Magnetic resonance imaging-based brain morphometry: development and application to normal subjects. *Ann Neurol* 25:61–67.
- Geschwind N, Levitsky W (1968) Human brain: left-right asymmetries in temporal speech region. *Science* 161:186–187.
- Kimura D (1993) Oxford psychology series, No 20, Neuromotor mechanisms in human communication. New York: Clarendon.
- Lancaster JL, Eberly D, Alyassin A, Downs JH III, Fox PT (1992) A geometric model for measurement of surface distance, surface area, and volume from topographic images. *Med Phys* 19:419–431.
- McLean PD, Newman JD (1988) Role of midline frontocortical cortex in production of the isolation call of squirrel monkeys. *Brain Res* 450:111–123.
- Morecraft RJ, Van Hoesen GW (1992) Cingulate input to the primary and supplementary motor cortices in the rhesus monkey: evidence for somatotopy in areas 24c and 23c. *J Comp Neurol* 322:471–489.
- Muakkassa KF, Strick PL (1979) Frontal lobe inputs to primate motor cortex: evidence for four somatotopically organized "premotor" areas. *Brain Res* 177:176–182.
- Ono M, Kubik S, Abernathy CD (1990) Atlas of the cerebral sulci. Stuttgart: Thieme.
- Pardo JV, Pardo PJ, Janer KW, Raichle ME (1990) The anterior cin-

- gulate cortex mediates processing selection in the Stroop attentional conflict paradigm. *Proc Natl Acad Sci USA* 87:256-259.
- Paus T, Petrides M, Evans AC, Meyer E (1993) Role of the human anterior cingulate cortex in the control of oculomotor, manual, and speech responses: a positron emission tomography study. *J Neurophysiol* 70:453-469.
- Rademacher J, Galaburda AM, Kennedy DN, Filipek PA, Caviness VS Jr (1992) Human cerebral cortex: localization, parcellation, and morphometry with magnetic resonance imaging. *J Cogn Neurosci* 4:352-374.
- Rademacher J, Caviness VS Jr, Steinmetz H, Galaburda AM (1993) Topographical variation of the human primary cortices: implications for neuroimaging, brain mapping, and neurobiology. *Cereb Cortex* 3:313-329.
- Raichle ME (1987) Circulatory and metabolic correlates of brain function in normal humans. In: *Handbook of physiology*, Sec 1, Vol 5, The nervous system (Mountcastle VB, ed), pp 643-674. Bethesda MD: American Physiological Society.
- Retzius G (1896) *Das Menschenhirn*. Stockholm: Norstedt Soner.
- Sanides F (1964) Structure and function of the human frontal lobe. *Neuropsychologia* 2:209-219.
- Sarkissov SA, Filimonoff JN, Kononova EP, Preobraschenskaja IS, Kukuev LA (1955) *Atlas of the cytoarchitectonics of the human cerebral cortex*. Moscow: Medzig.
- Smith GE (1907) A new topographical survey of the human cerebral cortex, being an account of the distribution of the anatomically distinct cortical areas and their relationship to the cerebral sulci. *J Anat Physiol* 41:237-254.
- Smith WK (1941) Vocalization and other responses elicited by excitation of the regio cingularis in the monkey. *Am J Physiol* 133:451-452.
- Steinmetz H, Volkman J, Jancke L, Freund HJ (1991) Anatomical left-right asymmetry of language-related temporal cortex is different in left- and right-handers. *Ann Neurol* 29:315-319.
- Sutton D, Larson C, Lindeman RC (1974) Neocortical and limbic lesion effects on primate phonation. *Brain Res* 71:61-75.
- Talairach J, Tournoux P (1988) *Co-planar stereotactic atlas of the human brain: 3-dimensional proportional system: an approach to cerebral imaging*. Stuttgart: Thieme.
- Talairach J, Szikla G, Tournoux P (1967) *Atlas d'anatomie stereotaxique du telencephale; etudes anatomo-radiologiques*. Paris: Masson.
- Taylor SF, Kornblum S, Minoshima S, Oliver LM, Koeppe RA (1994) Changes in medial cortical blood flow with a stimulus-response compatibility task. *Neuropsychologia* 32:249-255.
- Tomaiuolo F, Paus T, Morris R, MacDonald D, Petrides M, Evans AC (1993) Inter-individual variability of the sulcal pattern in the anterior cingulate region. *Soc Neurosci Abstr* 19:998.
- Vannier MW, Brunsden BS, Hildebolt CF, Falk D, Cheverud JM, Figiel GS, Perman WH, Kohn LA, Robb RA, Yoffie RL, Bresina SJ (1991) Brain surface cortical sulcal lengths: quantification with three-dimensional MR imaging. *Radiology* 180:479-484.
- Vogt BA, Barbas H (1988) Structure and connections of the cingulate vocalization region in the rhesus monkey. In: *The physiological control of mammalian vocalization* (Newman JD, ed), pp 203-225. New York: Plenum.
- Vogt C, Vogt O (1919) Allgemeinere Ergebnisse unserer Hirnforschung. *J Psychol Neurol* 25:279-462.
- Weinberg R (1905) Die Gehirnform der Polen. *Z Morphol Anthropol* 8:123-214, 279-424.
- Zilles K, Armstrong E, Moser KH, Schleicher A, Stephan H (1989) Gyrification in the cerebral cortex of primates. *Brain Behav Evol* 34:143-150.